

## Temperature dependent transient surface photovoltage spectroscopy of a $\text{Cu}_{1.95}\text{Zn}_{1.1}\text{Sn}_{0.96}\text{Se}_4$ kesterite single phase powder

Th. Dittrich, L. E. Valle Rios, S. Kapil, G. Gurieva, N. Rujisamphan, and S. Schorr

Citation: *Appl. Phys. Lett.* **110**, 023901 (2017); doi: 10.1063/1.4973539

View online: <http://dx.doi.org/10.1063/1.4973539>

View Table of Contents: <http://aip.scitation.org/toc/apl/110/2>

Published by the [American Institute of Physics](http://www.aip.org)

---

### Articles you may be interested in

[Optical properties of  \$\text{Cu}\_2\text{ZnSn}\(\text{SxSe}\_{1-x}\)\_4\$  solar absorbers: Spectroscopic ellipsometry and ab initio calculations](#)  
*Appl. Phys. Lett.* **110**, 021905021905 (2017); 10.1063/1.4973353

[Modification of defects and potential fluctuations in slow-cooled and quenched  \$\text{Cu}\_2\text{ZnSnSe}\_4\$  single crystals](#)  
*Appl. Phys. Lett.* **121**, 065704065704 (2017); 10.1063/1.4975483


[Discrepancy between integral and local composition in off-stoichiometric  \$\text{Cu}\_2\text{ZnSnSe}\_4\$  kesterites: A pitfall for classification](#)

*Appl. Phys. Lett.* **110**, 043901043901 (2017); 10.1063/1.4974819

[Structural transitions of ordered kesterite-type  \$\text{Cu}\_2\text{ZnSnS}\_4\$  under pressure](#)

*Appl. Phys. Lett.* **110**, 041905041905 (2017); 10.1063/1.4974941

---



Small Conferences. BIG Ideas.

Applied Physics  
Reviews

SAVE THE DATE!  
**3D Bioprinting: Physical and Chemical Processes**  
May 2–3, 2017 • Winston Salem, NC, USA

# Temperature dependent transient surface photovoltage spectroscopy of a $\text{Cu}_{1.95}\text{Zn}_{1.1}\text{Sn}_{0.96}\text{Se}_4$ kesterite single phase powder

Th. Dittrich,<sup>1</sup> L. E. Valle Rios,<sup>2</sup> S. Kapil,<sup>2</sup> G. Gurieva,<sup>2</sup> N. Rujisamphan,<sup>3</sup> and S. Schorr<sup>2,4</sup>

<sup>1</sup>Helmholtz-Zentrum Berlin für Materialien und Energie, Institut für Silizium-Photovoltaik, Kekuléstr. 5, D-12489 Berlin, Germany

<sup>2</sup>Helmholtz-Zentrum Berlin für Materialien und Energie, Abteilung Struktur und Dynamik von Energiematerialien, Hahn-Meitner-Platz 1, D-14109 Berlin, Germany

<sup>3</sup>Department of Physics, Faculty of Science, King Mongkuts University of Technology Thonburi, 10140 Bangkok, Thailand

<sup>4</sup>Institute of Geological Sciences, Freie Universität Berlin, Malteserstr. 74-100, D-12249 Berlin, Germany

(Received 9 November 2016; accepted 20 December 2016; published online 13 January 2017)

An off-stoichiometric but single phase  $\text{Cu}_{1.95}\text{Zn}_{1.1}\text{Sn}_{0.96}\text{Se}_4$  kesterite powder was investigated by temperature dependent transient surface photovoltage (SPV) spectroscopy. SPV signals excited at different wavelengths were transformed into SPV spectra that depended on the response time of measurement. Shallow electronic states and states with transition energies at 0.83 eV or 0.78... 0.9 eV were distinguished. The temperature dependence of the band gap of  $\text{Cu}_{1.95}\text{Zn}_{1.1}\text{Sn}_{0.96}\text{Se}_4$  was obtained. Results were discussed on the basis of defects in Cu-poor and Zn-rich kesterite. © 2017 Author(s). All article content, except where otherwise noted, is licensed under a Creative Commons Attribution (CC BY) license (<http://creativecommons.org/licenses/by/4.0/>). [<http://dx.doi.org/10.1063/1.4973539>]

Knowledge about defect states and the temperature dependence of the band gap ( $E_g$ ) of  $\text{Cu}_2\text{ZnSnSe}_4$  (CZTSe) and related kesterite materials is of practical and fundamental interest regarding applications in solar cells<sup>1,2</sup> and a deeper understanding of the structure<sup>3</sup> and defects<sup>4,5</sup> of CZTSe. The band gap of CZTSe is about 1 eV and depends sensitively on preparation conditions<sup>6</sup> and defects.<sup>4</sup> Order-disorder effects in the Cu-Zn layers of CZTSe have been shown by neutron and X-ray diffraction<sup>7</sup> and influenced  $E_g$  as well.<sup>8</sup> Recently,  $E_g$  of CZTSe was measured by spectral dependent ellipsometry over a wide temperature range<sup>9</sup> whereas defect states were not considered in the analysis. In  $\text{Cu}_2\text{ZnSn}(\text{S},\text{Se})_4$  (CZTSSe) kesterite based solar cells, the open circuit voltage is mainly limited by tail states<sup>10</sup> and the highest solar energy conversion efficiency can be reached for Zn-rich absorbers.<sup>11</sup> Further, off-stoichiometric but single phase kesterite has been discovered for Zn-rich but Cu-poor CZTSe.<sup>12</sup>

In this work, defect states and the temperature dependence of  $E_g$  in an offstoichiometric  $\text{Cu}_{1.95}\text{Zn}_{1.1}\text{Sn}_{0.96}\text{Se}_4$  single phase kesterite powder have been investigated by transient surface photovoltage (SPV) spectroscopy. In this method, surface photovoltage (SPV) transients are excited at numerous photon energies and the SPV values at fixed response time(s) are converted into spectra. Therefore, photo-generated electrons and holes can be excited over a large variety of optical transitions including delocalized and localized states (see Figure 1). The relaxation of charge carriers separated in space sensitively depends on defects states involved. The transient SPV spectroscopy allows, in contrast to conventional SPV spectroscopy<sup>13</sup> investigated with a Kelvin probe under cw illumination<sup>14</sup> or with a fixed capacitor under modulated light,<sup>15–17</sup> to distinguish spectral fingerprints of processes with relaxation times between ten(s) of ns and ms.

The investigated  $\text{Cu}_{1.95}\text{Zn}_{1.1}\text{Sn}_{0.96}\text{Se}_4$  powder was prepared by a reaction in a closed quartz tube (see Ref. 12 for details). For SPV measurements, a part of a glass substrate coated with  $\text{SnO}_2:\text{F}$  was covered with a carbon pad. The  $\text{Cu}_{1.95}\text{Zn}_{1.1}\text{Sn}_{0.96}\text{Se}_4$  powder was crumbled onto the carbon pad and fixed by slight pressing with a clean glass plate. After that, all parts of the powder which were not fixed at the

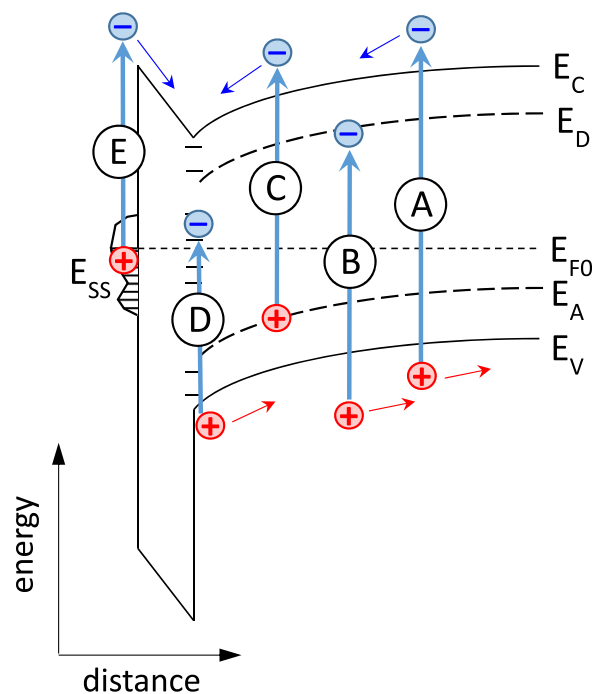


FIG. 1. Optical transitions near a semiconductor surface with a thin surface layer and directions of separation of photo-generated electrons or holes (A: band-to-band, B: valence band-to-donor, C: acceptor-to-conduction band, D: valence band-to-interface states, and E: surface state-to-conduction band). Trapping at localized states specifically limits the relaxation of charge carriers separated in space.

carbon pad were removed from the sample by shaking the glass substrate.

SPV transients were measured in the fixed capacitor arrangement<sup>13</sup> whereas the capacitor was formed between the carbon pad with the fixed  $\text{Cu}_{1.95}\text{Zn}_{1.1}\text{Sn}_{0.96}\text{Se}_4$  powder covered with a mica sheet and the quartz electrode coated with  $\text{SnO}_2\text{:F}$ . SPV transients were excited with pulses (duration time 5 ns) of a tunable Nd:YAG laser (EKSPLA, NT 342/1/UVE) at wavelengths between 720 and 2260 nm. SPV transients were recorded with a sampling oscilloscope (GAGE, CS14200, used sampling rate of 100 Ms/s) by applying a logarithmic read-out<sup>18</sup> and averaging over 40 transients at each wavelength (repetition rate 1 Hz). The temperature was varied between  $-120$  and  $120^\circ\text{C}$ . The pressure in the home-made chamber was  $3 \times 10^{-6}$  mbar. As remark, SPV signals disappeared irreversibly during heating at  $140^\circ\text{C}$ .

Figure 2 shows SPV transients excited with photon energies slightly above the band gap of  $\text{Cu}_{1.95}\text{Zn}_{1.1}\text{Sn}_{0.96}\text{Se}_4$  and measured at different temperatures. The sign of the SPV signals was negative at short times and changed to positive at longer times for measurements at lower temperatures. The SPV signals at 20 ns (after switching on the laser pulse,  $\Delta t_1$ ) were  $-30.5$  mV ( $-80$  and  $0^\circ\text{C}$ ) and  $-27$  mV ( $80^\circ\text{C}$ ) and still increased slightly at times longer than  $\Delta t_1$  within tens of ns at low temperatures.

A negative sign of SPV signals corresponds to preferential separation of photo-generated electrons towards the external surface. Fast charge separation is dominated by charge transport in a surface space charge region. Therefore, the grains of the investigated  $\text{Cu}_{1.95}\text{Zn}_{1.1}\text{Sn}_{0.96}\text{Se}_4$  powder can be considered as a p-type semiconductor. The change of the sign of the SPV signals at longer times gave evidence for trapping of holes at surface states or de-trapping of electrons from states close to the external surface. The further increase of SPV signals in time corresponds to an increase in the distance between the centers of positive and negative photo-generated charge, probably due to electron transport within a very thin region near the surface with a high density of defects.

The SPV transients decayed faster with increasing temperature for temperatures below  $80^\circ\text{C}$ . For example, the

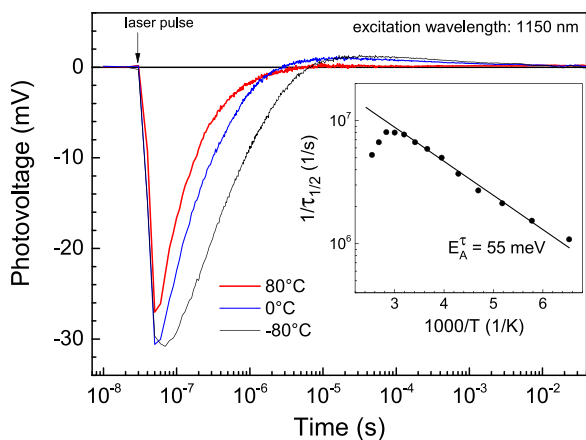


FIG. 2. SPV transients measured at  $-80$ ,  $0$ , and  $80^\circ\text{C}$  (thin black, medium blue, and thick red lines, respectively) of a  $\text{Cu}_{1.95}\text{Zn}_{1.1}\text{Sn}_{0.96}\text{Se}_4$  powder sample excited at a wavelength of  $1150$  nm. The arrow marks the onset of the laser pulse. The inset shows the Arrhenius plot of the reciprocal time at which the signal decreased to half.

times at which the SPV signals decreased to the half amplitude ( $\tau_{1/2}$ ) were about  $0.44$ ,  $0.14$ , and  $0.09 \mu\text{s}$  for  $-80$ ,  $0$ , and  $80^\circ\text{C}$ , respectively. The activation energy of the reciprocal  $\tau_{1/2}$  ( $E_A^\tau$ ) was about  $55$  meV. This low value of  $E_A^\tau$  points to the importance of shallow states such as the copper vacancy ( $V_{\text{Cu}}$ )<sup>4</sup> for the relaxation of large negative SPV signals.

SPV transients measured at  $-120^\circ\text{C}$  and excited at different wavelengths are presented in Figure 3. The SPV signals at  $\Delta t_1$  were  $-26.5$ ,  $-11$ ,  $-2.7$ , and  $-0.7$  mV for excitation at  $1100$ ,  $1200$ ,  $1410$ , and  $2010$  nm, respectively. Therefore, the SPV signals decreased strongly in the region of  $E_g$  of  $\text{Cu}_{1.95}\text{Zn}_{1.1}\text{Sn}_{0.96}\text{Se}_4$  (between  $1200$  and  $1410$  nm) but did not disappear for excitation with photon energies significantly lower than  $E_g$ . The latter can be explained by excitation of mobile charge carriers from defect states. The change of the sign from negative to positive disappeared for the SPV transient excited at  $2010$  nm, which gave evidence for direct excitation of, for example, electrons from occupied defect states near the external surface to un-occupied states in the bulk.

The inset of Figure 3 shows SPV spectra converted at response times of  $0.02$ ,  $0.1$ ,  $1$ ,  $10$ , and  $100 \mu\text{s}$  ( $\Delta t_1$  to  $\Delta t_5$ , respectively) in a wide spectral range. The SPV signals at  $\Delta t_1$  and  $\Delta t_2$  were very similar, amounted to about  $-1$  mV even at the lowest photon energies, increased to  $-3.8$  mV between  $0.83$  and  $0.90$  eV, decreased practically to zero at  $0.97$  eV and increased strongly to  $-34$  mV between about  $1.00$  eV and  $1.10$  eV, i.e., near the band gap. The SPV signals at  $\Delta t_3$  amounted as well to about  $-1$  mV at the lowest photon energies, increased slightly to  $-1.4$  mV at around  $0.83$  eV, changed the sign at about  $0.92$  eV, reached  $+2.2$  mV at  $0.96$  eV, changed the sign again around  $1.01$  eV, and reached about  $-16$  mV at  $1.1$  eV. For  $\Delta t_4$  and  $\Delta t_5$ , no SPV signals were observed at the lowest photon energies, the SPV signals set on at about  $0.83$  eV ( $\Delta t_4$ ) and  $0.76$  eV ( $\Delta t_5$ ) and increased

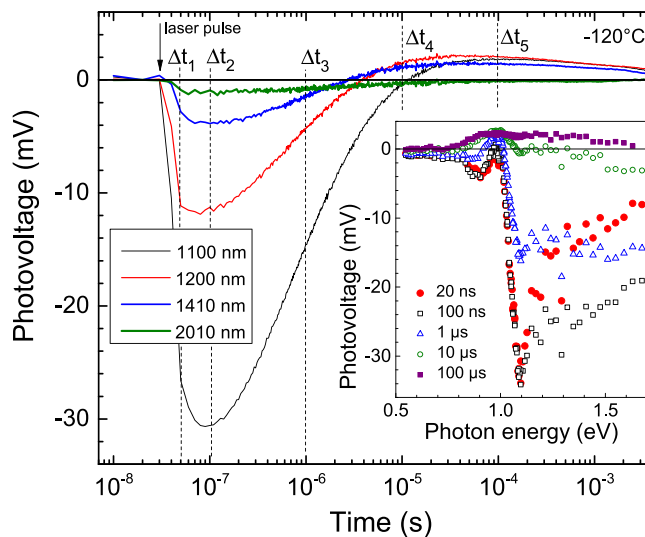


FIG. 3. SPV transients of a  $\text{Cu}_{1.95}\text{Zn}_{1.1}\text{Sn}_{0.96}\text{Se}_4$  powder sample measured at  $-120^\circ\text{C}$  and excited at wavelengths of  $1100$ ,  $1200$ ,  $1410$ , and  $2010$  nm (thin black, medium red, thick blue, and thick green lines, respectively). The arrow marks the onset of the laser pulse. The dashed lines mark the times at which SPV signals of transients measured at different wavelengths were transformed to spectra. The inset shows the corresponding SPV spectra between  $0.53$  and  $1.72$  eV obtained at  $20$  ns,  $100$  ns,  $1 \mu\text{s}$ ,  $10 \mu\text{s}$ , and  $100 \mu\text{s}$  after the onset of the laser pulse (filled circles, open squares, open triangles, open squares, and filled squares, respectively).

to +2.2 mV at +2.6 mV at 0.96 eV ( $\Delta t_4$ ) and 0.93 eV ( $\Delta t_5$ ). The SPV signals at  $\Delta t_4$  changed to only  $-0.5$  mV near the band gap. In contrast, the SPV signals at  $\Delta t_5$  did not show a signature of the band gap.

The transition setting on at around 1.00 eV corresponds to the band gap of the  $\text{Cu}_{1.95}\text{Zn}_{1.1}\text{Sn}_{0.96}\text{Se}_4$  kesterite phase. The transition at 0.83 eV can be assigned to  $\text{Zn}_{\text{Sn}}$  if regarding the excess of Zn and the energy obtained from theoretical studies.<sup>4</sup> The low SPV signals setting on at the lowest photon energies can be related to defects deeper in the band gap such as tin vacancies ( $\text{V}_{\text{Sn}}$ )<sup>4</sup> or zinc interstitials ( $\text{Zn}_i$ )<sup>4</sup> or to surface states. The transition setting on between 0.79 and 0.83 eV led to an opposite sign of the SPV signals and to very long relaxation times, i.e., charge separation was not related to the surface space charge region in this case. The reason for transitions leading to SPV signals with a positive sign is probably a very thin defect layer with distributed trap states near the surface. Depending on the thickness of a related defect layer, an upward band bending very close to the surface can be a reason for the change of the sign of the SPV signals. Band bending at CZTSSe/CdS interfaces<sup>19</sup> or at grain boundaries between CZTSSe crystallites,<sup>20</sup> for example, has been demonstrated by photoelectron spectroscopy<sup>19</sup> or KPFM (Kelvin probe force microscopy), respectively.<sup>20</sup>

Figure 4 shows the negative values of the SPV signals measured at 20 ns for  $-100$  and  $120^\circ\text{C}$  in a spectral range between 0.97 and 1.07 eV. The investigation of the temperature dependence of the band gap ( $E_g(T)$ ) of  $\text{Cu}_{1.95}\text{Zn}_{1.1}\text{Sn}_{0.96}\text{Se}_4$  kesterite in terms of the onset energy or of a Tauc gap<sup>21</sup> is vague due to the superposition of different processes. The region near the  $E_g$  had to be approximated by a superposition of a Gaussian with a temperature-independent peak energy ( $E_t$  about 0.992–0.993 eV) and a temperature-dependent onset of fundamental absorption ( $E_{\text{on}}$  about 1.008 and 0.995 at  $-100$  and  $120^\circ\text{C}$ , respectively).

The Arrhenius plot of the amplitude of the Gaussian is given in Figure 5. The thermally activated part resulted in an

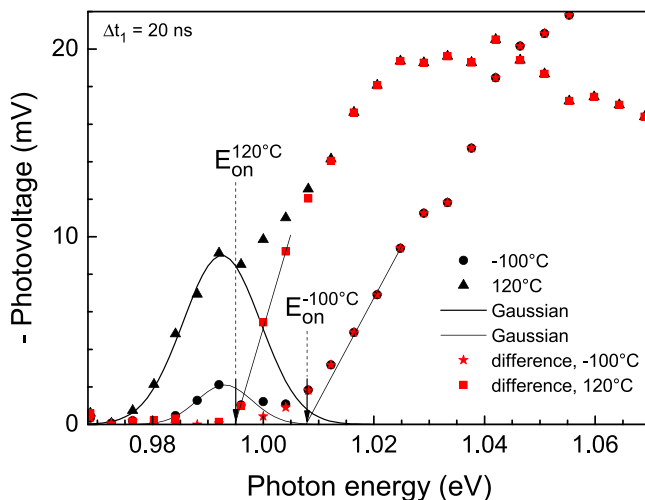


FIG. 4. Negative transient SPV spectra near the band edge obtained at 20 ns for  $-100$  (circles) and  $120^\circ\text{C}$  (triangles). The spectra were approximated by Gaussians fixed in energy (thin and thick solid lines for  $-100$  and  $120^\circ\text{C}$ , respectively) and parts shifting towards higher energy with increasing temperature (stars and squares for  $-100$  and  $120^\circ\text{C}$ , respectively) where the arrows mark the onset energies.

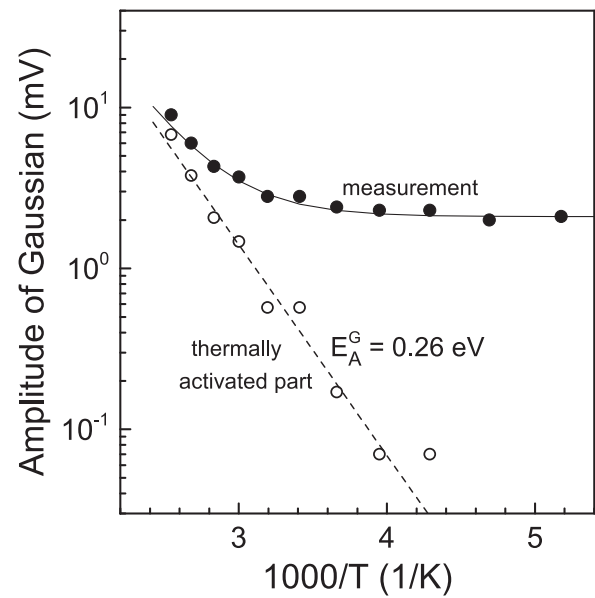


FIG. 5. Arrhenius plot of the measured SPV amplitudes of the Gaussians (solid circles) and of the thermally activated part (empty circles). The activation energy was 0.26 eV.

activation energy  $E_A^G$  equal to about 0.26 eV. This means that the defect state with the optical transition at  $E_t$  is coupled with a transfer of charge from or into a deep state the occupation of which is thermally activated. The state at  $E_t$  and the deep state are probably related to the same but differently charged defect.

The value of  $E_{\text{on}}$  can be practically treated as the band gap of  $\text{Cu}_{1.95}\text{Zn}_{1.1}\text{Sn}_{0.96}\text{Se}_4$  kesterite. The temperature dependence of  $E_{\text{on}}$  of  $\text{Cu}_{1.95}\text{Zn}_{1.1}\text{Sn}_{0.96}\text{Se}_4$  kesterite is compared with the temperature dependence of  $E_g$  of  $\text{Cu}_2\text{ZnSnSe}_4$  kesterite (values of  $E_g$  after Choi *et al.*<sup>9</sup>) in Figure 6. The values of  $E_{\text{on}}$  of  $\text{Cu}_{1.95}\text{Zn}_{1.1}\text{Sn}_{0.96}\text{Se}_4$  kesterite are larger than those of  $E_g$  of  $\text{Cu}_2\text{ZnSnSe}_4$  kesterite. Up to about  $50^\circ\text{C}$ , the decrease in  $E_{\text{on}}$  of  $\text{Cu}_{1.95}\text{Zn}_{1.1}\text{Sn}_{0.96}\text{Se}_4$  kesterite with increasing temperature was only  $-0.08$  meV/K, which was

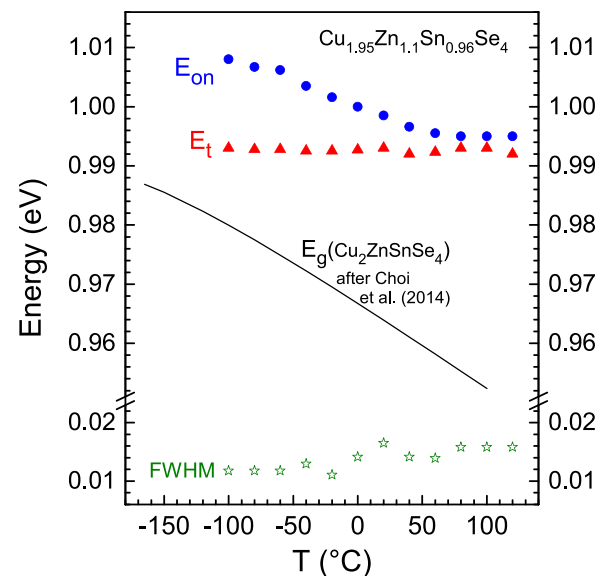


FIG. 6. Temperature dependencies of the onset energy (circles), of the peak and full width at half maximum of the Gaussians (triangles and stars, respectively) in comparison to the band gap of  $\text{Cu}_2\text{ZnSnSe}_4$  (solid line, after Ref. 9).



much less than for the temperature dependent decrease in  $E_g$  of  $\text{Cu}_2\text{ZnSnSe}_4$  kesterite (about  $-0.13$  meV/K) in the considered range. At temperatures above  $50^\circ\text{C}$ , the values of  $E_{\text{on}}$  tended to saturate around  $0.955$  eV which was close to  $E_i$ . In addition, the full width at half maximum of the Gaussian tended to increase from about  $12$  to  $16$  meV in the temperature range between  $-50$  and  $50^\circ\text{C}$ . Therefore, the temperature dependence of  $E_{\text{on}}$  of  $\text{Cu}_{1.95}\text{Zn}_{1.1}\text{Sn}_{0.96}\text{Se}_4$  kesterite was strongly influenced by defect states near the band gap. For comparison, high concentrations of different defect pairs can strongly influence  $E_g$  of kesterites as well.<sup>4</sup>

Electronic transitions in crystallites of a  $\text{Cu}_{1.95}\text{Zn}_{1.1}\text{Sn}_{0.96}\text{Se}_4$  single phase kesterite powder have been studied by temperature dependent transient surface photovoltage spectroscopy. This method allows distinguish shallow and deep electronic states in relation to the relaxation time of charge carriers separated in space. Electronic transitions could be correlated with results of theoretical analysis on defects in Cu poor but Zn rich kesterite.<sup>4</sup> The bandgap of  $\text{Cu}_{1.95}\text{Zn}_{1.1}\text{Sn}_{0.96}\text{Se}_4$  kesterite was higher than for  $\text{Cu}_2\text{ZnSnSe}_4$  kesterite and the temperature dependence of  $E_{\text{on}}$  of  $\text{Cu}_{1.95}\text{Zn}_{1.1}\text{Sn}_{0.96}\text{Se}_4$  kesterite was lower than for  $\text{Cu}_2\text{ZnSnSe}_4$  kesterite. The analysis of defect states by transient surface photovoltage spectroscopy and their deeper understanding will be useful not only for the further improvement of kesterite solar cells but also for the investigation of any other photoactive material.

<sup>1</sup>See, for example, T. K. Thodorov, J. Tang, S. Bag, O. Gunawan, T. Gokmen, Y. Zhu, and D. B. Mitzi, *Adv. Energy Mater.* **3**, 34 (2013).

- <sup>2</sup>X. Liu, Y. Feng, H. Cui, F. Liu, X. Hao, G. Conibeer, D. B. Mitzi, and M. Green, *Prog. Photovoltaics: Res. Appl.* **24**, 879 (2016).
- <sup>3</sup>C. Persson, *J. Appl. Phys.* **107**, 053710 (2010).
- <sup>4</sup>S. Chen, A. Walsh, X.-G. Gong, and S.-H. Wie, *Adv. Mater.* **25**, 1522 (2013).
- <sup>5</sup>M. Kumar, A. Dubey, N. Adikari, S. Venkatesan, and Q. Qiao, *Energy Environ. Sci.* **8**, 3134 (2015).
- <sup>6</sup>S. Ahn, S. Jung, J. Gwak, A. Cho, K. Shin, K. Yoon, D. Park, H. Cheong, and J. H. Yun, *Appl. Phys. Lett.* **97**, 021905 (2010).
- <sup>7</sup>S. Schorr, *Sol. Energy Mater. Sol. Cells* **95**, 1482 (2011).
- <sup>8</sup>G. Rey, A. Redinger, J. Sendler, T. P. Weiss, M. Thevenin, M. Guennou, B. El Adib, and S. Siebentritt, *Appl. Phys. Lett.* **105**, 112106 (2014).
- <sup>9</sup>S. G. Choi, T. J. Kim, S. Y. Hwang, J. Li, C. Persson, Y. D. Kim, S.-H. Wei, and I. L. Repins, *Sol. Energy Mater. Sol. Cells* **130**, 375 (2014).
- <sup>10</sup>T. Gokmen, O. Gunawan, T. K. Todorov, and D. B. Mitzi, *Appl. Phys. Lett.* **103**, 103506 (2013).
- <sup>11</sup>W. Wang, M. T. Winkler, O. Gunawan, T. Gokmen, T. K. Todorov, Y. Zhu, and D. B. Mitzi, *Adv. Energy Mater.* **4**, 1301465 (2014).
- <sup>12</sup>L. E. Valle Rios, K. Neldner, G. Gurieva, and S. Schorr, *J. Alloys Compd.* **657**, 408 (2016).
- <sup>13</sup>L. Kronik and Y. Shapira, *Surf. Sci. Rep.* **37**, 1 (1999).
- <sup>14</sup>J. Lagowski, I. Baltov, and H. Gatos, *Surf. Sci.* **40**, 216 (1973).
- <sup>15</sup>V. Duzhko, V. Yu. Timoshenko, F. Koch, and Th. Dittrich, *Phys. Rev. B* **64**, 075204 (2001).
- <sup>16</sup>X. Z. Lin, T. Dittrich, S. Fengler, M. C. Lux-Steiner, and A. Ennaoui, *Appl. Phys. Lett.* **102**, 143903 (2013).
- <sup>17</sup>T. Dittrich, C. Awino, P. Prajontat, B. Rech, and M. Ch. Lux-Steiner, *J. Phys. Chem. C* **119**, 23968 (2015).
- <sup>18</sup>Th. Dittrich, S. Bönisch, P. Zabel, and S. Dube, *Rev. Sci. Instrum.* **79**, 113903 (2008).
- <sup>19</sup>R. Haight, A. Barkhouse, O. Gunawan, B. Shin, M. Copel, M. Hopstaken, and D. B. Mitzi, *Appl. Phys. Lett.* **98**, 253502 (2011).
- <sup>20</sup>G. Y. Kim, J. R. Kim, W. Jo, D.-H. Son, D.-H. Kim, and J.-K. Kang, *Nanosci. Res. Lett.* **9**, 10 (2014).
- <sup>21</sup>J. Tauc, *Mater. Res. Bull.* **3**, 37 (1968).